NACA Publications on Aircraft Icing Cylinders

For the SAE AC-9C Aircraft Icing Technology Committee, April 6, 2022

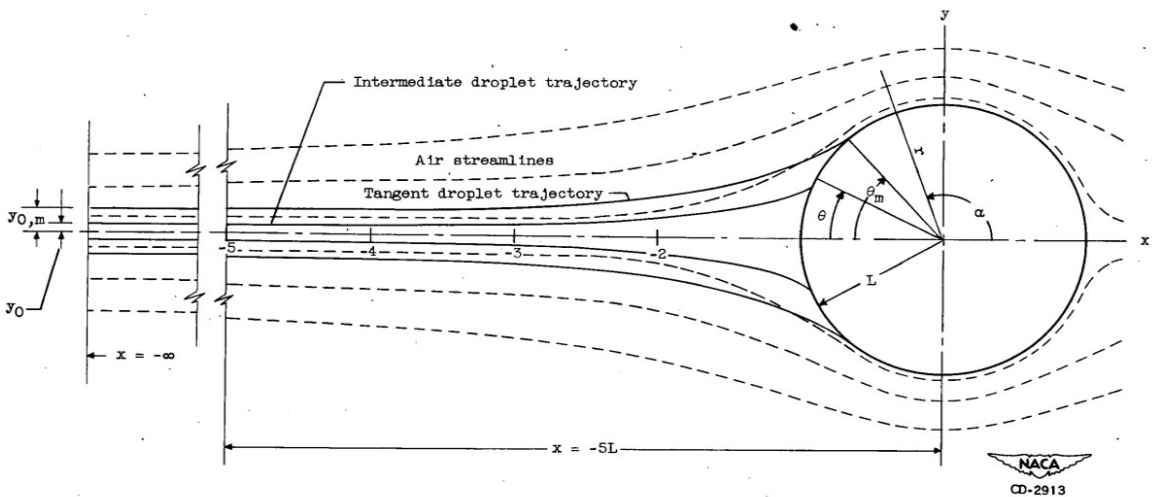

Figure 1. - Coordinate system for cylinder.

icinganalysis@gmail.com

The NACA Icing Publications

NACA (National Advisory Committee for Aeronautics, 1915 to 1958) was a predecessor to NASA.

NACA published 132+ publications on aircraft icing (next slide)

The publications are still cited in recent icing publications, including:

- “Engineering Summary of Airframe Icing Technical Data”, FAA ADS-4, 1969 (half of the references are NACA publications)
- “Ice, Frost, and Rain Protection” SAE (original publication 1969)
- “The Aircraft Icing Handbook”, DOT/FAA, 1991
- CFR 14, Chapter 25, Appendix C (regularly updated)

My mentors were well versed in the NACA publications.

There are still technical uses for the data today.

There is a website
https://icinganalysis.github.io/index.html

Subject Categories

The 16 categories of the 132 publications

- Meteorology of Icing Clouds
- Fundamental Properties of Water
- Meteorological Instruments
- Impingement of Cloud Drops
- Propeller Ice Protection
- Induction System Ice Protection
- Turbine-Type Engine and Inlets
- Wing Ice Protection
- Windshield Ice Protection
- Cooling Fan Ice Protection
- Radome Ice Protection
- Antenna Icing
- Inlet and Vent Ice Protection
- Jet Penetration
- Heat Transfer
- Miscellaneous

Cylinders were selected as a topic that includes several categories

"The meteorological data obtained with the multicylinder method are the only data available for the design of ice-protection equipment for aircraft" *NACA-RM-E53D23*

"The collection of ice by the cylinders is similar to the collection of ice by airplane components." *von Glahn, Uwe H.: The Icing Problem, presented at Ottawa AGARD Conference. AG 19/P9, June 10-17 1955*

Multicylinders

Much of the NACA era icing flight data were obtained with multicylinder instruments, particularly MVD.

NACA-TN-2708

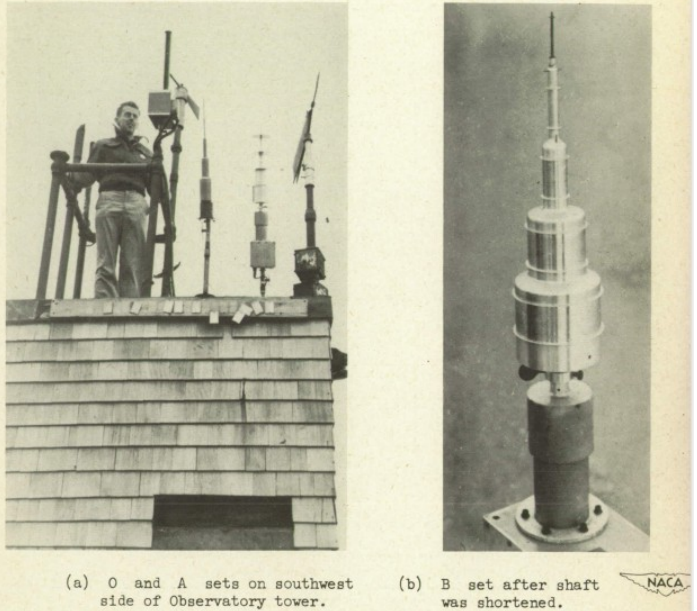

(a) O and A sets on southwest side of Observatory tower. (b) B set after shaft was shortened.

Figure 1.- Multicylinder cloud meters used in comparative study at Mount Washington Observatory.

NACA-RM-E52D23

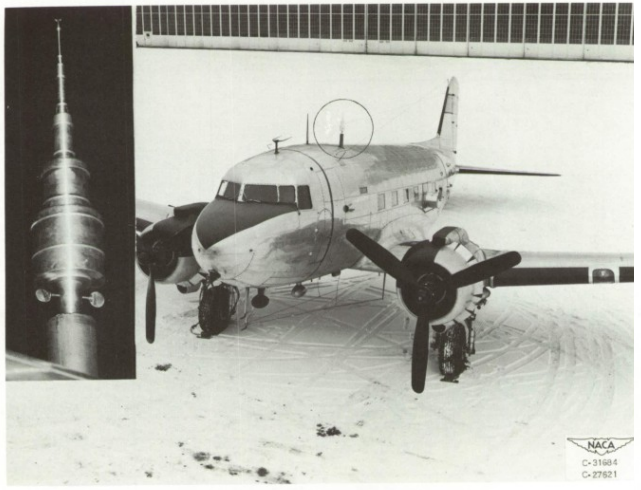

Figure 1. - Rotating multicylinder set extended through top of airplane fuselage.

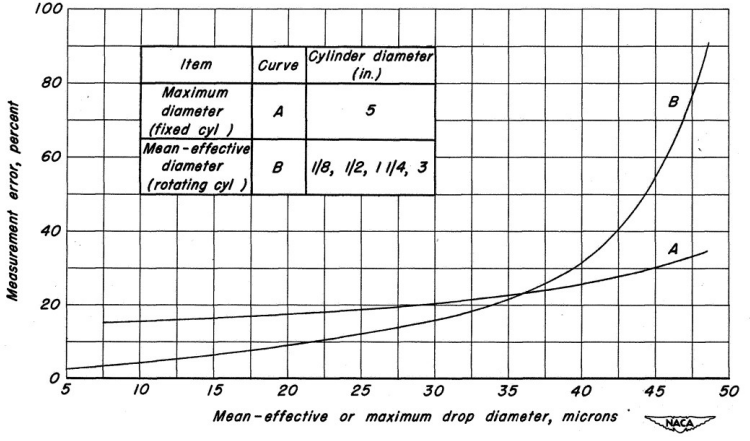

Figure 7.-Calculated error in the measurement of mean-effective drop diameter with four rotating cylinders, and maximum drop diameter with one nonrotating cylinder. Calculations based on assumption of errors of ± 5% in determining the weight of ice accretions on the rotating cylinders, and + 5° in the determination of the angle of water impingement (θ_m) on the nonrotating cylinder.

NACA-TN-1904

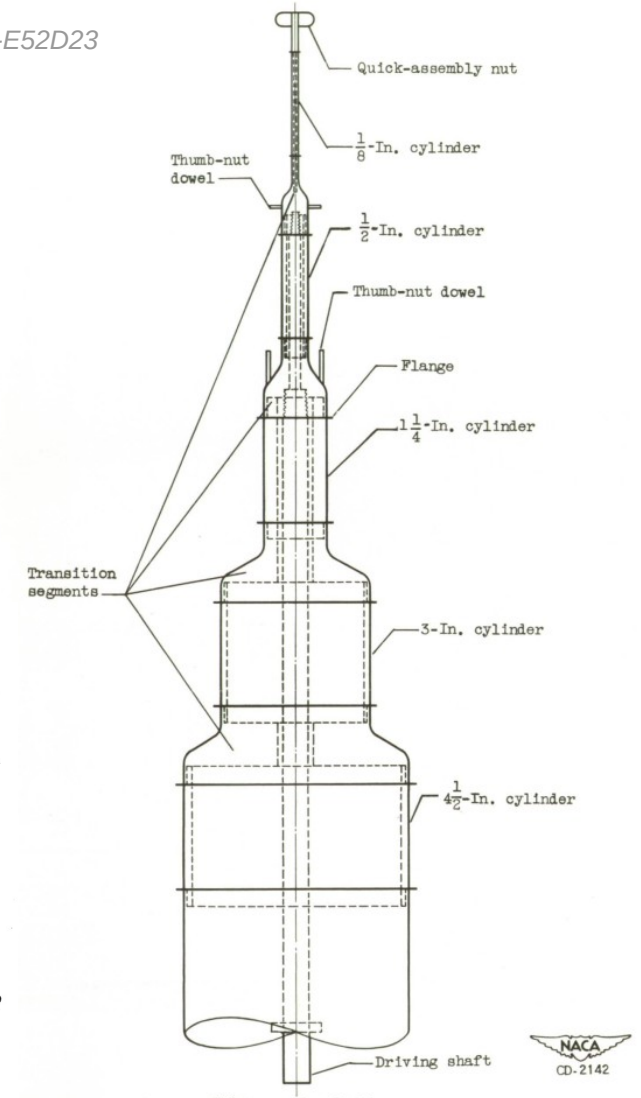

(a) Assembly sketch.

Figure 3. - Assembled set of cylinders.

Publications in the Cylinder Thread

NACA-TN-779 “Aerodynamic Heating and Deflection of Drops by an Obstacle in an Airstream in Relation to Aircraft Icing"
AAF-TR-5418 “Mathematical Investigation of Water Droplet Trajectories”, Langmuir and Blodgett
NACA-TN-1393 “A Flight Investigation of the Meteorological Conditions Conducive to the Formation of Ice on Airplanes"
NACA-TN-1424 "A Further Investigation of the Meteorological Conditions Conducive to Aircraft Icing"
NACA-RM-A9C09 "A Review of Instruments Developed for the Measurement of the Meteorological Factors Conducive to Aircraft Icing"
NACA-TN-1904 "Observations of Icing Conditions Encountered in Flight During 1948"
NACA-TN-2708 "Comparison of Three Multicylinder Icing Meters and Critique of Multicylinder Method"
NACA-TN-2903 "Impingement of cloud droplets on aerodynamic bodies as affected by compressibility of air flow around the body"
NACA-TN-2904 "Impingement of water droplets on a cylinder in an incompressible flow field and evaluation of rotating multicylinder method for measurement of droplet-size distribution, volume-median droplet size, and liquid-water content in clouds"
NACA-RM-E53D23 "Procedure for Measuring Liquid-Water Content and Droplet Sizes in Super-cooled Clouds by Rotating Multicylinder Method"
NACA-TR-1215 "Impingement of Cloud Droplets and Procedure for Measuring Liquid-Water Content and Droplet Sizes in Supercooled Clouds by Rotating Multicylinder Method"
NACA-TN-3338 "A Dye-Tracer Technique for Experimentally Obtaining Impingement Characteristics of Arbitrary Bodies and a Method for Determining Droplet Size Distribution"

Most publications are available at https://ntrs.nasa.gov/

Reviews

"... the recommendation was made that before attacking what appeared to be a new icing problem we should study the icing work of the 1940's and 50's."
John J. Reinmann, NASA-TM-81651, 1979

The reviews condense the icing publications into an approximately 10 minute read each.

A typical review format is:

- a quote from the paper
- a one-line summary
- key points
- the Abstract (in searchable text form, not just a pdf image)
- a detailed discussion, including key figures
- executable Python code (in some cases) to reproduce the results
- how the publication got used, and where it is cited
- where to find the publication (most, but not not all, are on the NASA NTRS site)
- the references the publication cited (in searchable text)

What is still used in the post-NACA era

Langmuir Drop Size Distributions

Icing physics terminology (K, Ko, MVD)

Cylinder impingement correlations

Cylinder as an approximation of an airfoil leading edge

Icing conditions in regulations

Cylinder icing thermodynamics for icing indication and detection

Langmuir Distributions

The variation of atmospheric cloud water drop diameters is high. Since the MED or MVD is the median drop diameter, water drops having larger diameters than the MED or MVD exist. NACA researchers used the Langmuir distribution in table I-1 to calculate MED for the data used to define 14 CFR parts 25, Appendix C and 29, Appendix C icing conditions (Reference I4). So, the Langmuir distribution is used to describe the variation of 14 CFR parts 25, Appendix C and 29, Appendix C cloud drop diameters. Since drops larger than the MVD exist, consider using the Langmuir D distribution with the 50 µm maximum median drop diameter of 14 CFR arts 25, Appendix C and 29, Appendix C to determine impingement limits.

TABLE IX

Four Assumed Distributions of Droplet Size

Liquid Water Content Per cent	a/a_0 B	$(a/a_0)^{1.5}$ C	$(a/a_0)^{2.0}$ D	$(a/a_0)^{2.5}$ E
5	0.56	0.42	0.31	0.23
10	0.72	0.61	0.52	0.44
20	0.84	0.77	0.71	0.65
30	1.00	1.00	1.00	1.00
20	1.17	1.26	1.37	1.48
10	1.32	1.51	1.74	2.00
5	1.49	1.81	2.22	2.71

Langmuir and Blodgett

Table I-1. Langmuir Distributions

Fractional Liquid Water Content in Each Size Group ~ %	Langmuir Distribution ~ (Drop Diameter)/Median Drop Diameter				
	A	B	C	D	E
5	1.00	0.56	0.42	0.31	0.23
10	1.00	0.72	0.61	0.52	0.44
20	1.00	0.84	0.77	0.71	0.65
30	1.00	1.00	1.00	1.00	1.00
20	1.00	1.17	1.26	1.37	1.48
Fractional Liquid Water Content in Each Size Group ~ %	**Langmuir Distribution ~ (Drop Diameter)/Median Drop Diameter**				
	A	B	C	D	E
10	1.00	1.32	1.51	1.74	2.00
5	1.00	1.49	1.81	2.22	2.71

https://www.faa.gov/documentLibrary/media/Advisory_Circular/AC_20-73A.pdf

Terminology

Langmuir and Blodgett

$$K = \lambda_s / C, \tag{10}$$

where C is the radius of the cylinder and λ_s is the "Range" which the droplet would have as a projectile released in still air with the velocity U, assuming that Stokes' law holds. The advantage of using this quantity, which has the dimensions of a length, is that it permits us to put the equations into convenient form.

The value of λ_s is given by

$$\lambda_s = (2/9)\varrho_s a^2 U/\eta, \tag{11}$$

$$K = 2\varrho_s a^2 U/9\eta C. \tag{12}$$

TABLE I

Values of $C_D R/24$ and λ/λ_s as Functions of R. The values of $C_D R/24$ calc. were obtained by means of Eq. (22)

R	$C_D R/24$	$C_D R/24$ Calc.	λ/λ_s	R	$C_D R/24$	$C_D R/24$ Calc.	λ/λ_s
0.00	1.00	1.00	1.00	200	6.52	6.94	0.2668
0.05	1.009		0.9956	250	7.38		0.2424
0.1	1.018		0.9911	300	8.26		0.2234

$$(K_0 - 1/8) = (\lambda/\lambda_s)\,(K - 1/8). \tag{40}$$

From DOT/FAA/CT-88/8-1

$$K = \frac{1}{18}\,\frac{\delta^2\, V_\infty\, \rho_w}{c\, \mu_a} \tag{2-6}$$

$$K_0 = K\left(\frac{\lambda}{\lambda_s}\right) \tag{2-8}$$

TABLE 2-3. CHARACTERISTIC LENGTHS FOR SEVERAL BODIES FOR CALCULATION OF K_0

BODY	CHARACTERISTIC LENGTH	DATA SOURCE
Airfoil	Chord, c	All airfoil data
Cylinder	Radius, D/2	NACA Rpt. 1215 (Reference 2-32)

$$K_0 = 18\,K\left[Re^{-2/3} - \frac{\sqrt{6}}{Re}\,\text{Arctan}\,\frac{Re^{1/3}}{\sqrt{6}}\right] \tag{2-10}$$

Be very careful about units and dimensions when using K and Ko!

Cylinder Impingement Correlations

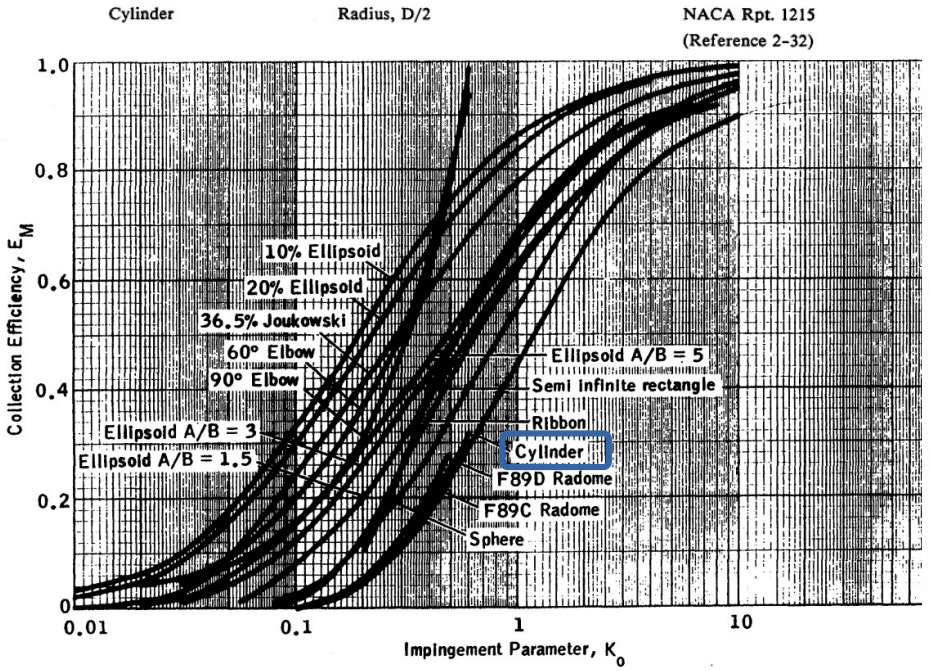

From DOT/FAA/CT-88/8-1

FIGURE 2-44. COLLECTION EFFICIENCY VERSUS K_o FOR GEOMETRIC BODIES - THEORETICAL DATA FOR 0° ANGLE OF ATTACK

in Table V of L & B, the collection efficiency is given by:

$$E = 0.457 (\log_{10} 8K_o)^{1.634}$$

For higher values of K (i.e. $K > 3.0$) use is made of Langmuir's parameter H_E, defined by:

$$H_E = 1 + 0.5708 (C_D Re/24) - 0.73 \times 10^{-4} Re_d^{1.38} \quad \text{(L \& B eqn. 43)}$$

Values of $C_D Re/24$ as a function of Re are given in Table I of Langmuir and Blodgett, together with the empirical equation:

$$C_D Re/24 = 1 + 0.197 Re^{0.63} + 2.6 \times 10^{-4} Re^{1.38} \quad \text{(L \& B eqn. 22)}$$

Greater accuracy in the range of Reynolds number $20 \leq Re_d \leq 500$ is afforded by a slight modification to this equation, as follows:

$$C_D Re/24 = 1 + 0.212 Re^{0.6} + 2.6 \times 10^{-4} Re^{1.38}$$

whence $$H_E = \pi/2 + 0.121 Re_d^{0.6} + 0.754 \times 10^{-4} Re_d^{1.38}$$

Finally, the collection efficiency is given by:

$$E = K/(K + H_E) \quad \text{(L \& B eqn. 42)}$$

From LTR-LT-92, "An Appraisal of the Single Rotating Cylinder Method for Liquid Water Content Measurement"

Cylinder approximation for airfoil leading edge

In equation (3.3), K is the non-dimensional inertia parameter defined by Langmuir and Blodgett[8] as

$$K = \frac{\rho_w \delta^2 V}{18 d \mu_a} \qquad (3.5)$$

In Langmuir and Blodgett's paper the cylinder radius was used in place of the dimension d. Thus, for cylinders, the radius should be used in equation (3.5). Bragg[6] and Ruff[7] used a length c which they defined as a characteristic dimension. Airfoil chord is commonly used in evaluating the inertia parameter for aircraft icing applications. For scaling, however, the use of chord means that for a general trajectory analysis the same inertia parameter could result for airfoils of the same chord but different forms, whether thick or thin. By setting d to twice the leading-edge radius, this problem is avoided. Maximum airfoil thickness might also be considered for the characteristic length, but the use of twice the leading-edge radius leads to collection efficiencies consistent with those from the LEWICE ice-accretion code,[9] as will be shown below.

3.3.1. Langmuir and Blodgett Trajectory Analysis

Langmuir and Blodgett's expression for modified inertia parameter is

$$K_0 = \frac{1}{8} + \frac{\lambda}{\lambda_{Stokes}}\left(K - \frac{1}{8}\right), \text{ for } K > \frac{1}{8} \qquad (3.8)$$

$$(K_0 - 1/8) = (\lambda/\lambda_s)\,(K - 1/8). \qquad (40)$$

Langmuir and Blodgett

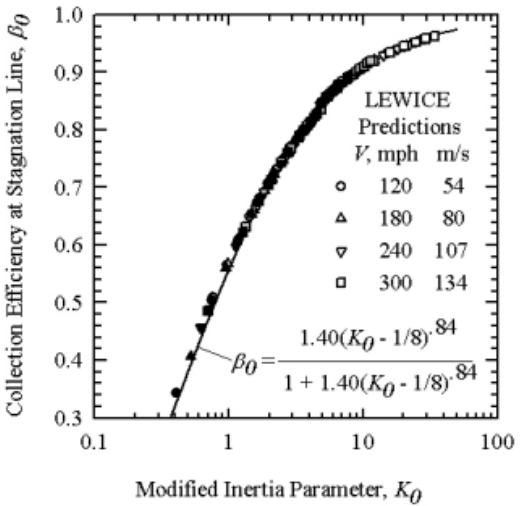

Figure 3.3.2.—Stagnation Collection Efficiency for NACA 0012 Airfoils at 0° Angle of Attack. Static Temperature, 10°F; Static Pressure, 14 psia; Airspeed, 120 to 300 mph; Water Drop Median Volume Diameter, 10 to 50 μm; Liquid-Water Content, 1 g/m^3. Open Symbols, 7-in Chord; Shaded Symbols, 21-in Chord; Solid Symbols, 31.5-in Chord. Data Represented by Symbols are from LEWICE[9] Predictions.

From NASA-CR-2004-21875 "Manual of Scaling Methods"

Icing Regulations

FIGURE 1

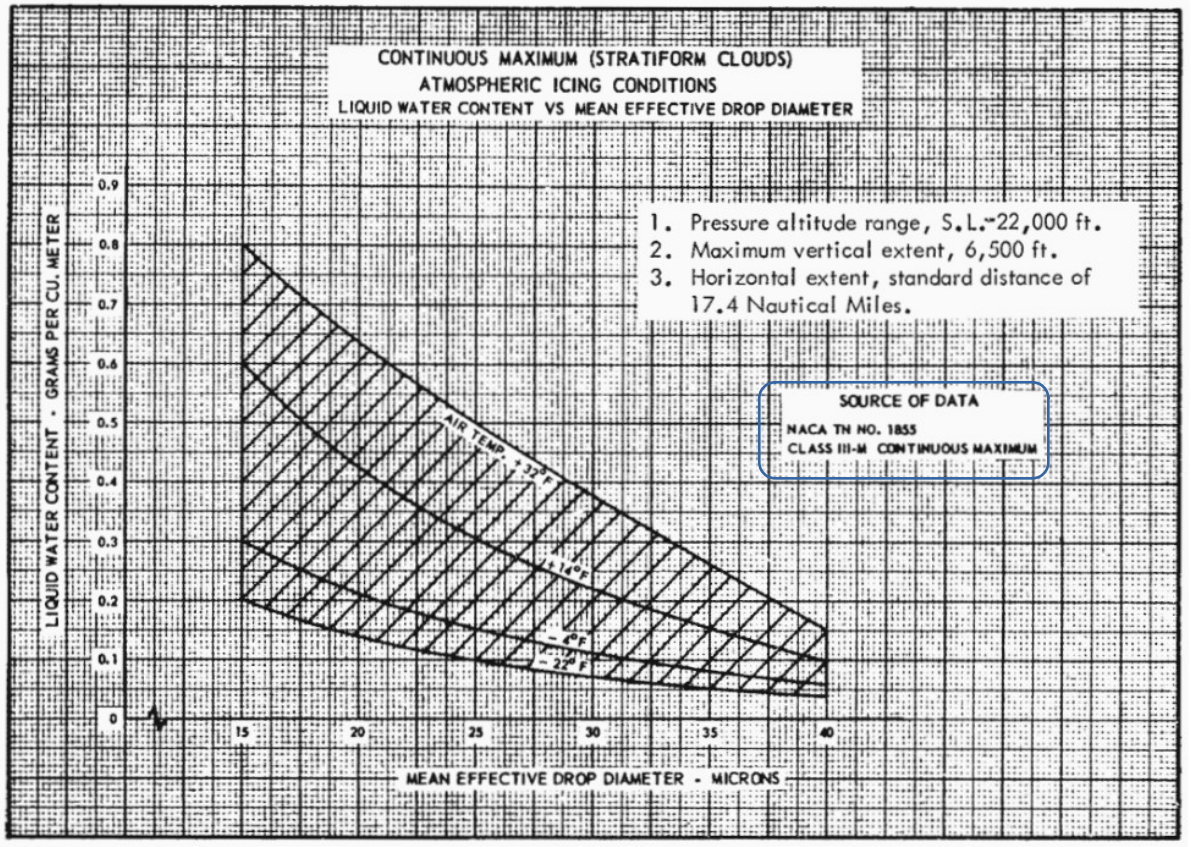

https://www.ecfr.gov/current/title-14/chapter-I/subchapter-C/part-25/appendix-Appendix%20C%20to%20Part%2025

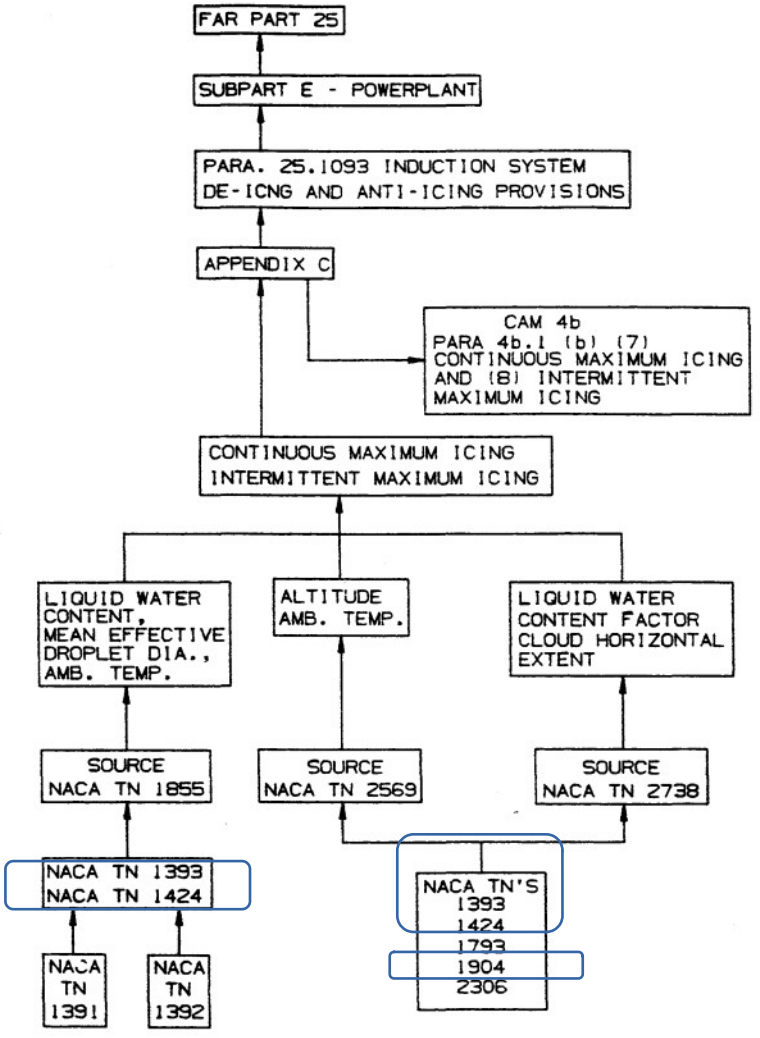

From DOT/FAA/CT-88/8-1

FIGURE 3-1. DERIVATION OF FAR ICING STANDARDS (REFERENCE 3-12)

Icing Thermodynamics

"Ludlam limit" *(will all impinging water freeze)* considerations are important for ice detection and LWC calibration

"The heat economy of a rimed cylinder", F. Ludlam, 1951

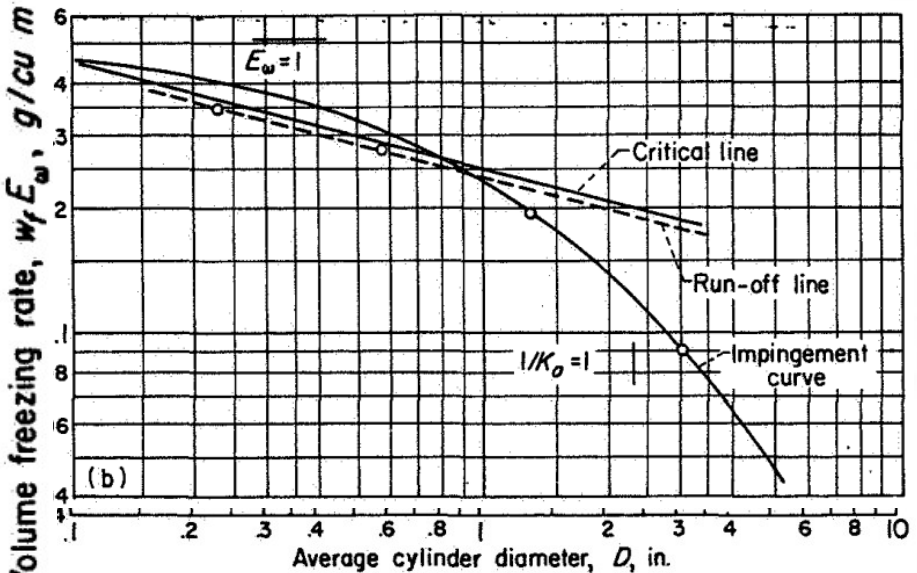

(a) No run-off from any cylinder [flight 20 (1/29/47, run 1), ref. 33].
(b) Run-off from two smallest cylinders, nearly continuous cloud [flight 10 (4/18/49, run 2), ref. 35].
(c) Run-off from two smallest cylinders, discontinuous cloud [flight 19 (2/9/50, run 2), ref. 35].
(d) Run-off from all four cylinders [flight 179 (3/29/48, run 17), ref. 36].

FIGURE 24.—Examples illustrating effect of run-off on multicylinder data.

NACA-TR-1215

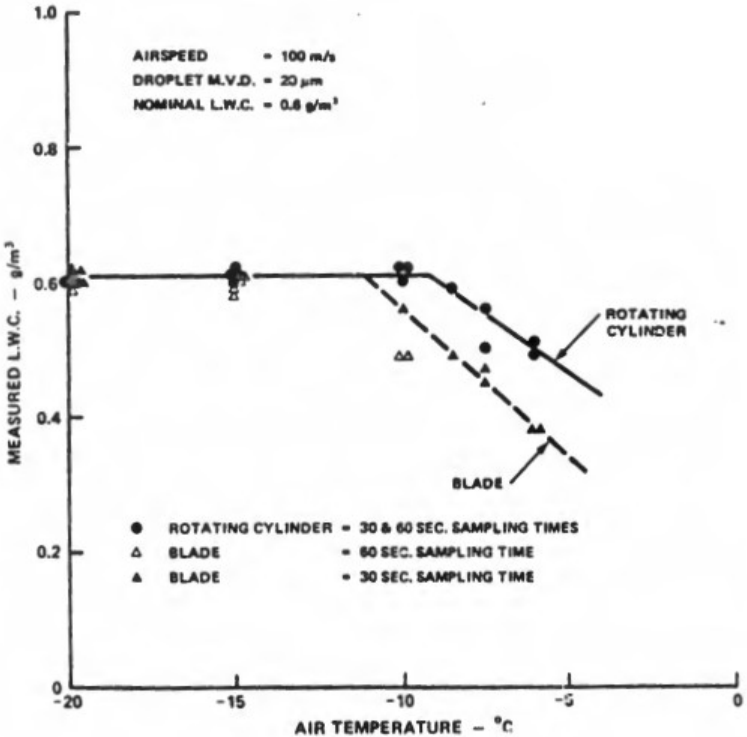

FIG. 3: EFFECT OF TEMPERATURE ON MEASURED VALUE OF LIQUID WATER CONTENT USING ROTATING CYLINDER AND BLADE METHODS

From LTR-LT-92, "An Appraisal of the Single Rotating Cylinder Method for Liquid Water Content Measurement"

Comparison to post-NACA cylinder impingement data

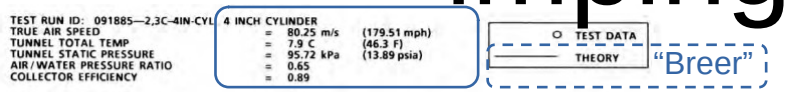

"Breer"

NASA-CR-4257, 1989

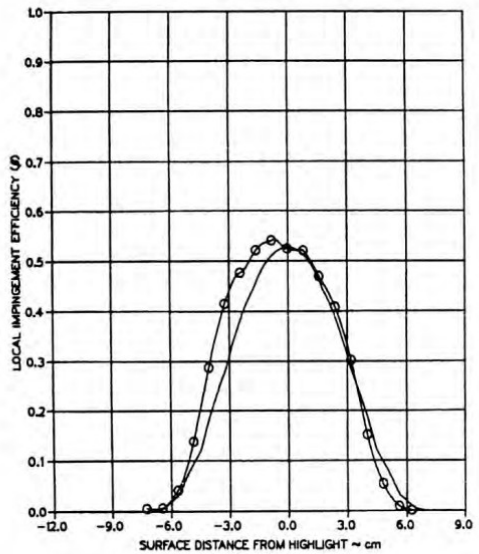

FIGURE 6.6

AVERAGED LOCAL WATER DROPLET IMPINGEMENT EFFICIENCY DATA FOR 4 INCH CYLINDER AND ICE SHAPES (MOUNTED ON 2 INCH CYLINDER)
PAGE 1 OF 5.

(Used 7-bin drop size distribution)

Each theory is within the test repeatability

Case Em values	20.36 MVD	16.45 MVD
Test average	0.38	0.26
Test +/-10% repeatability	0.42 0.34	0.29 0.23
Theory (Breer)	0.35	0.26
Langmuir and Blodgett (original)	0.35	0.25
Langmuir and Blodgett (corrected)	0.36	0.29
NACA-TN-2904	0.40	0.31

NACA-TN-2904 trends slightly higher than the other theory values

Lots of great images!

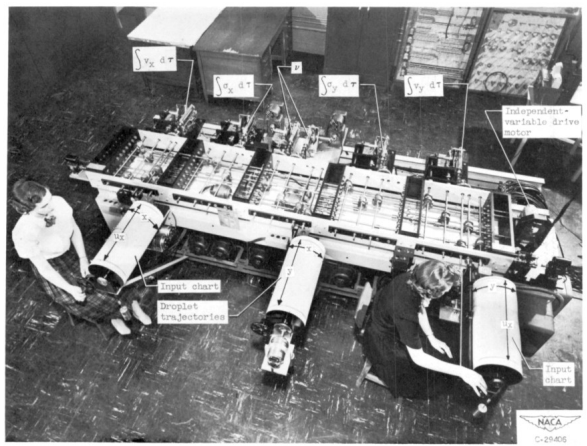

Figure 15. - Water-droplet-trajectory analog.

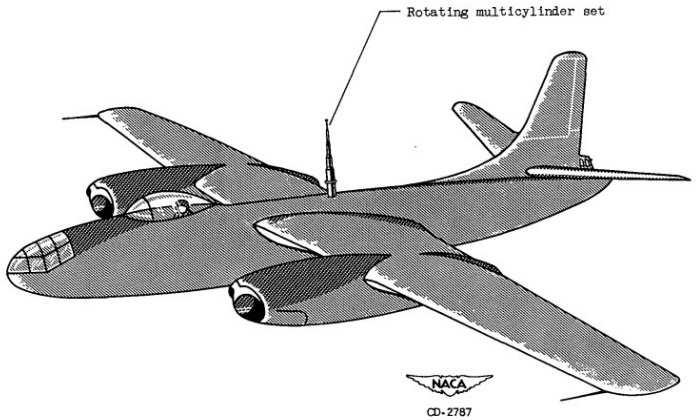

Figure 1. - Rotating multicylinder set extended through top of airplane fuselage.

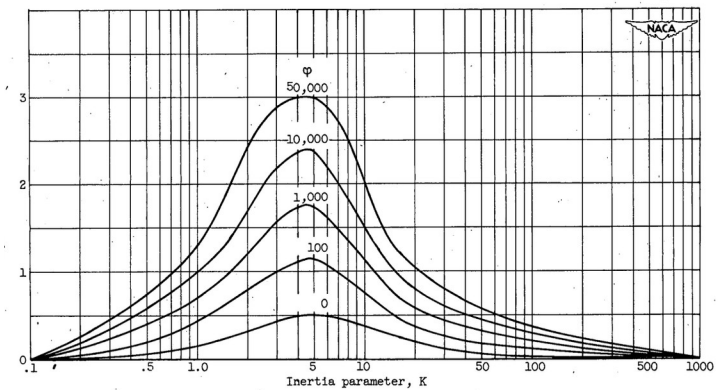

Figure 4. - Correction factor for compressibility effect.

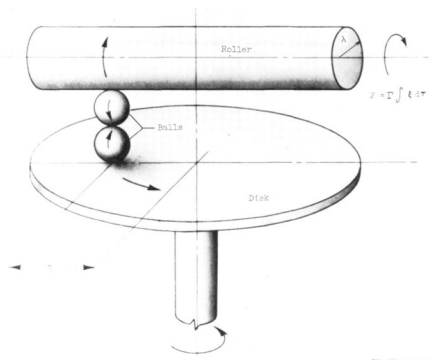

Figure 16. - Principle of integrator.

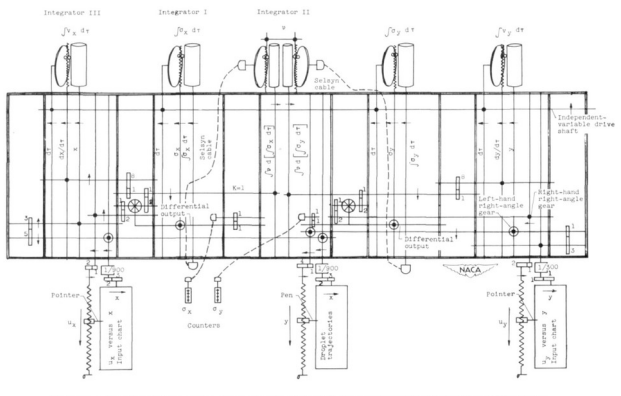

Figure 19. - Plan view of analog setup. Arrows indicate direction of shaft rotation or pen movement for positive sense.

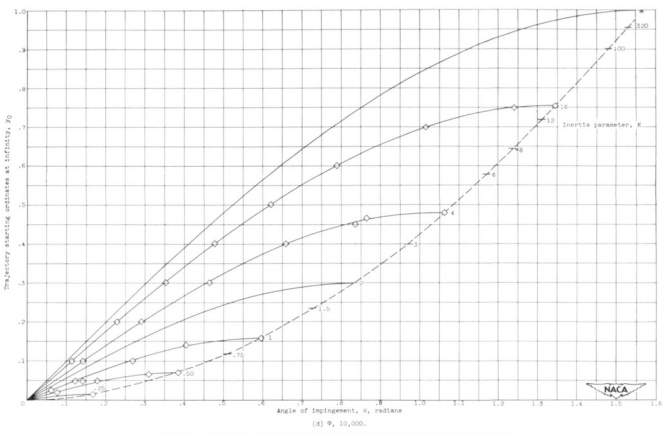

Figure 9. - Continued. Trajectory starting ordinates as function of angle of impingement

(d) Φ, 10,000.

Appendix

More general histories of NACA

Lew Rodert, Epistemological Liaison, and Thermal De-Icing at Ames
https://history.nasa.gov/SP-4219/Chapter2.html

"We Freeze to Please": A History of NASA's Icing Research Tunnel
https://ntrs.nasa.gov/citations/20020066162

"Bringing the Future Within Reach: the NASA John H. Glenn Research Center"
https://history.nasa.gov/SP-2016-627.pdf

Python Code

Code written in the Python programming language is available for many of the publications reviewed.

Methods described are implemented in modern code

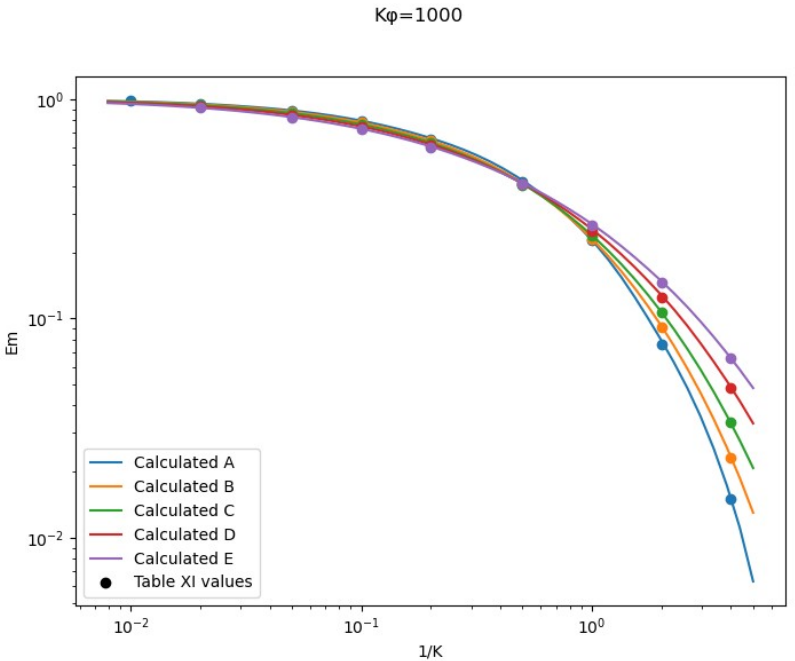

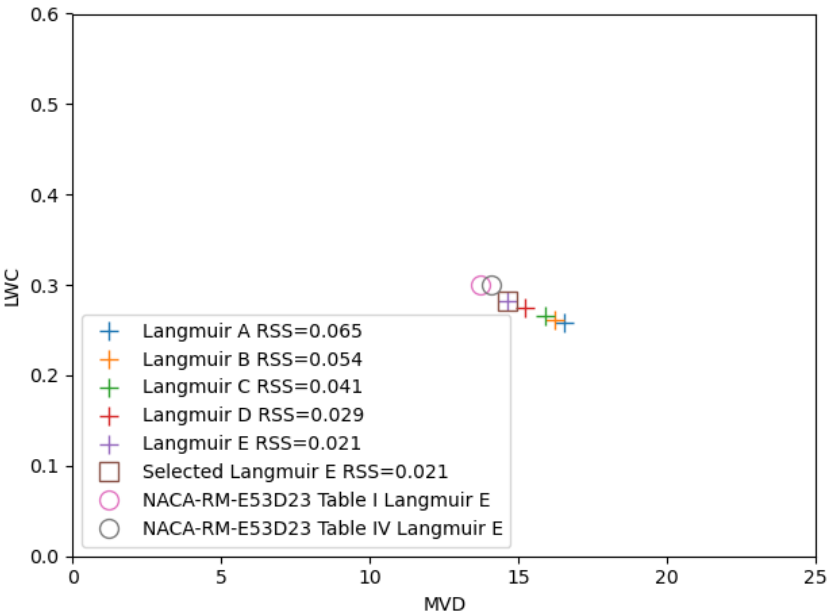

https://github.com/icinganalysis/icinganalysis.github.io, LGPL license

Origins of the Langmuir distributions

In our analysis (pages 264–265 of Part I) of the Houghton and Radford data on size distribution it was concluded that their measurements were correct when the covering fraction a was less than 0.1. In their paper they give a "volume distribution curve" (Fig. 7), based on the microphotograph of the Fig. 4 for which $a = 0.072$. As ordinates they plot the relative volumes (liquid water content, Δw) of the droplets for equal increments of droplet radius.

Super-cooled Water Droplets in Rising Currents of Cold Saturated Air 317

TABLE XXXII

Two Assumed Distributions of Droplet Size

Liquid Water Content Per cent	B		C	
	Radius %	Number %	Radius %	Number %
5	56	21	42	34
10	72	20	60	22
20	84	24	77	22
30	100	22	100	15
20	117	9	126	5
10	132	3	151	1.5
5	149	1	181	0.5

The distribution given under *C* in Table XXXI, and used for Curve *C* of Fig. 13, represents a wider spread of droplet sizes, obtained by choosing relative radii for the seven groups values equal to the 1.5th power of those of the *B* distribution.

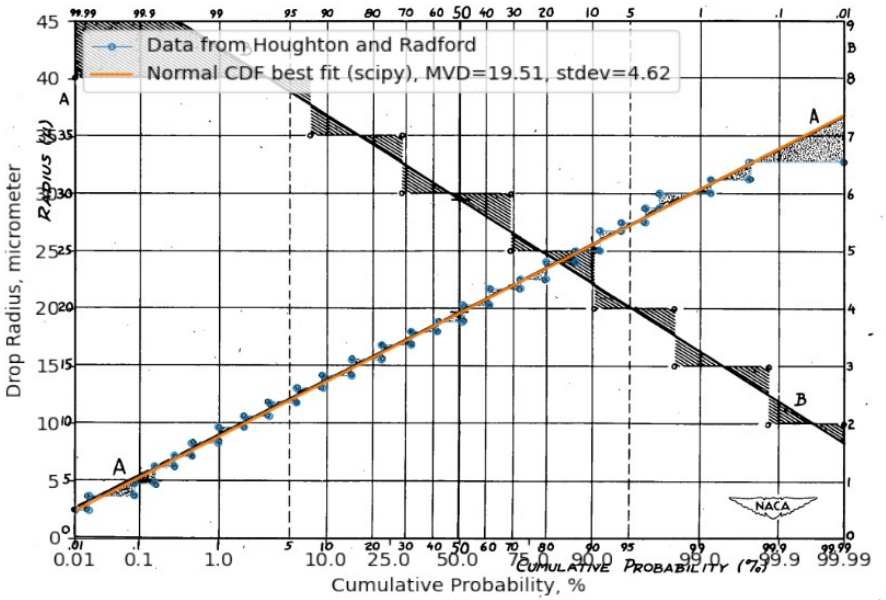

Figure 6.- Volume distribution of water in fog (A-A) according to Houghton and Radford (reference 13) and in cloud (B-B) according to Vonnegut, Cunningham, and Katz (reference 14). Horizontal line segments are interpreted according to the following example (curve B-B): Drops measuring 6 microns in radius, to the nearest micron, correspond to the range between 31 and 72 percent cumulative liquid water content. Sloping lines are the best-fitted normal distributions and shading is for emphasis only.

NACA TN 2708

37

https://icinganalysis.github.io/a-langmuir-b-drop-size-distribution-is-almost-a-normal-distribution.html

Why not just use LEWICE?

For **rotating** cylinders, LEWICE may not yield results similar to NACA-TR-1215 for cases where all of the water does not freeze.

There are several potential reasons for this:

- While LEWICE is well validated [1] for airfoils, there is less data for cylinders, and much less for rotating cylinders
- NACA-TR-1215 uses a different heat transfer coefficient than LEWICE
- LEWICE has a standing water model, which for some cylinder cases yields large amounts of water standing near the leading edge. In a rotating cylinder, this water would have an opportunity to rotate to a different location where freezing might be possible, but LEWICE does not have that capability.

For rotating cylinders, purpose built special analytical models for calculating the “Ludlam Limit” have generally been used [2].

1. Validation Results for LEWICE 2.0 https://ntrs.nasa.gov/citations/19990021235

2. Stallabrass J R: “An appraisal of the single rotating cylinder method of liquid water content measurements.” Canada. National Research Council. Report LTR-LT-92, 1978.

Abstract

Over 130 technical papers on aircraft icing were published by NACA (National Advisory Committee for Aeronautics, a predecessor to NASA, 1915 to 1958).

Three of these papers are specifically cited in current aircraft icing regulations. Numerous others are cited in design guides such as ADS-4, “Engineering Summary of Airframe Icing Technical Data”, and the DOT/FAA “Aircraft Icing Handbook”.

Selected NACA papers are reviewed in detailed, and, where applicable, Python code is used to reproduce the results. Important related, contemporary works, such a Langmuir and Blodgett’s “Mathematical Investigation of Water Drop Trajectories” are included.

This presentation will focus on the papers relating to multicylinder icing instruments, that were used to establish the current icing regulations.

Related website: https://icinganalysis.github.io